IEEE Photonics Journal
An IEEE Photonics Society Publication

Open Access

All-Fiber-Optics-Based Microwave Photonic Filter With Tunable Center Frequency and Passband Plus Notch

Volume 9, Number 5, October 2017

Xiao Zhang
Chengming Wang
Wenchao Liao
Wenxin Zhang
Shengnan Ai
Zhangkai Peng
Ping Xue

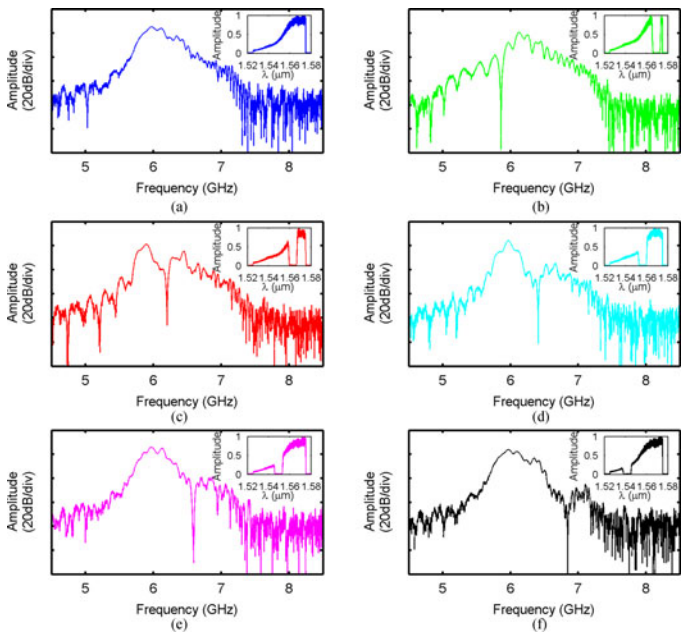

DOI: 10.1109/JPHOT.2017.2730587
1943-0655 © 2017 IEEE

IEEE photonics SOCIETY

IEEE

All-Fiber-Optics-Based Microwave Photonic Filter With Tunable Center Frequency and Passband Plus Notch

Xiao Zhang,[1] Chengming Wang,[2] Wenchao Liao,[2] Wenxin Zhang,[2] Shengnan Ai,[2] Zhangkai Peng,[2] and Ping Xue[2]

[1]State Key Laboratory of Low-dimensional Quantum Physics and Department of Physics, Tsinghua University and School of Life Science, Beijing Institute of Technology, Beijing 100081, China
[2]State Key Laboratory of Low-dimensional Quantum Physics and Center for Atomic and Molecular Nanoscience, Department of Physics, Tsinghua University and Collaborative Innovation Center of Quantum Matter, Beijing 100084, China

DOI:10.1109/JPHOT.2017.2730587

Manuscript received April 26, 2017; revised July 12, 2017; accepted July 17, 2017. Date of publication July 17, 2017; date of current version July 27, 2017. This work was supported in part by the National Natural Science Foundation of China under Grant 61227807 and Grant 61575108 and in part by Tsinghua Initiative Scientific Research Program under Grant 2013THZ02-3. Corresponding author: Ping Xue (e-mail: xuep@tsinghua.edu.cn).

Abstract: We propose and demonstrate a microwave photonic band-pass filter (MPF), which features a single light source, with continuously and independently tunable center frequency and bandwidth. The center frequency and bandwidth can be adjusted by tuning the variable optical delay line and the position of a spatial filter, respectively. Using a balanced photodetector, the baseband, which is ineradicable in some conventional designs, and the common-mode noise are canceled in our proof-of-concept experiment. Alternatively, a notch with continuously tunable frequency can also be added in the MPF. The experimental measurements of the frequency response of this MPF are demonstrated, which have a good agreement with the theoretical simulations.

Index Terms: Microwave photonic filter, single bandpass filter.

1. Introduction

For the supplementary advantages inherent to photonics such as low loss, high bandwidth, immunity to electromagnetic interference, wide tunability and high reconfigurability [1]–[3], microwave photonic filter (MPF) has been studied intensively during the recent years. The approaches of MPFs, based on a dispersive medium, a Mach-Zehnder interferometer and an electro-optic modulator, show simple structure, large tunability and potential high Q value [4]–[6]. However, the bandwidths are fixed in these MPFs [4]–[6] with tunable center frequencies only. In some practical applications, the center frequency and bandwidth of MPF are required to be tunable to meet the different demands. Therefore, we will present an improved design with tunable center frequency and bandwidth as well.

A number of MPFs with continuously and independently tunable bandwidth/center frequency have been demonstrated. Based on a single wavelength source, electro-optical phase modulator and a tunable optical filter via thermal tuning, a single pass-band MPF, with the capability of tuning the

center frequency and filter bandwidth independently, was presented [7]. However, the temperature control in thermal tuning [7] typically suffers from nonlinearity and slow response, due to the device's thermal capacity.

W. Li *et al.* presented a continuously tunable single-notch MPF achieved by interfering between a single passband MPF using a non-sliced amplified spontaneous emission source and a broadband microwave photonic phase shifter using a laser diode [8]. Based on a comb-based optical tapped delay line in a thermostatic periodically poled lithium niobate waveguide, a MPF with variable bandwidth, shape, and center-frequency was experimentally demonstrated [9]. Y. Yu *et al.* reported a kind of notch MPF achieved by an all-pass MPF minus a band-pass MPF in a balanced photodetector. The all-pass filter is based on a single-frequency light and the band-pass one is acquired by using the spectrum-sliced broadband optical source [10]. W. Li *et al.* experimentally demonstrated a band-pass/band-stop MPF using two tunable laser sources, an orthogonal phase modulation and an optical filtering [11]. However, all these designs [8]–[11] employ two light sources and therefore are not cost-effective.

For the MPFs based on stimulated Brillouin scattering, the bandwidth or center frequency can be tuned with a microwave signal generated by arbitrary waveform generator (AWG), which is applied to an optical modulator for pump light [12]–[14]. As everyone knows, the key advantage of microwave photonics technology is to use optics to achieve ultrahigh-speed signal processing which is difficult for electronics in microwave band. However, these MPFs [12]–[14] fail to follow this basic principle of microwave photonics and have to employ at least one radio frequency local oscillator and/or one AWG with a bandwidth of at least 1 GHz, which are too expensive for MPF in practical use.

In this paper, we propose and demonstrate a band-pass MPF, which features a single light source and no need of either temperature controller or AWG, with continuously tunable center frequency and bandwidth. Furthermore, a notch with continuously tunable frequency may also be added in the MPF as well. With a fiber-compatible optical filter, both the optical spectrum and the frequency response of the MPF can be achieved with instant and linear response. To eliminate the baseband which is ineradicable in some conventional designs [4], [15], [16], dual balanced detection is employed here. Theoretical analysis on the frequency response of this MPF is presented.

2. Experimental Setup and Theory

In conventional MPF, the optical spectrum, which is the carrier of microwave signal, is fixed. Therefore it somewhat limits the flexibility of MPF. In fact, more flexibility can be optically obtained by tuning the optical spectrum. In our improved design, by adding a flexibly adjustable optical filter we are able to modify the optical spectrum to achieve different MPF parameters as desired. The experimental setup of the proposed MPF is shown in Fig. 1(a). Low coherence CW light centered at 1550 nm with average power of 22 mW and bandwidth of $\sim$45 nm is generated by a superluminescent diode (SLD). The CW light is modulated by a 10 GHz bandwidth Mach-Zehnder modulator (MZM). The MZM is driven by input microwave signal generated by vector network analyzer (VNA). As dispersive medium, a fiber Bragg grating (FBG), which works in C-band, is employed after MZM. Then the light is sent to a tunable optical filter with resolution of $\sim$13 nm/mm. By tuning the spatial filter, the shape of filtered optical spectrum varies accordingly.

To measure the output optical spectrum from tunable optical filter, a 10:90 fiber coupler and an optical spectrum analyzer (OSA) are used. The filtered light goes through a Mach-Zehnder interferometer (MZI) and the optical path difference between two arms could be tuned by the variable optical delay line (VDL). For a balance of optical loss, two VDLs are used here. Finally, two outputs of interferometer are detected by a balanced amplified photodetector which is able to remove the common-mode noise and improve signal-to-noise ratio (SNR) of the system. The detected signal is sent back to VNA to measure the frequency response of the MPF. As shown in Fig. 1(b), the tunable optical filter consists of collimator, grating, lens, mirror and movable blocker as a spatial filter. The measured optical spectra after the SLD and the FBG are shown in Fig. 1(c).

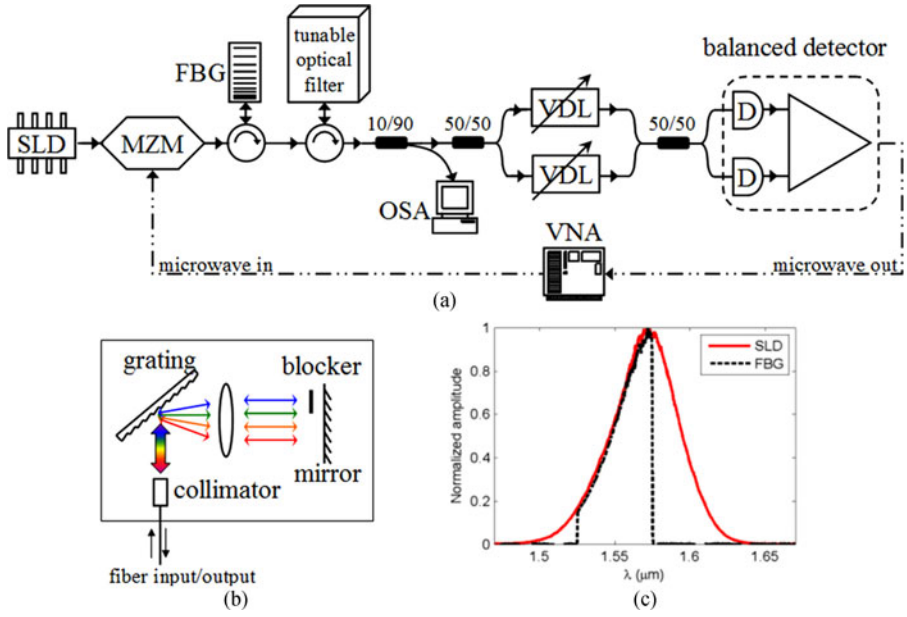

Fig. 1. (a) Schematic of the experimental setup of MPF. (b) Tunable optical filter architecture. (c) The optical spectra after the SLD and the FBG.

The complex electrical field at the output of SLD can be written as

$$\hat{E}(t) = \frac{1}{2\pi}\int_0^{+\infty} E(\Omega)\, e^{j\Omega t} d\Omega, \tag{1}$$

where Ω is the angular frequency of the light. The statistical property of $E(\Omega)$ is expressed as [17]

$$\left\langle E(\Omega) E^*(\Omega')\right\rangle = 2\pi N(\Omega)\,\delta(\Omega - \Omega'), \tag{2}$$

where $N(\Omega)$ is power spectral density (PSD) of light. Suppose that the light is modulated by MZM with a single-frequency microwave signal. Under small-signal condition, only two first-order sidebands are considered. The Fourier transform of complex electrical field after MZM is

$$E_{\mathrm{MZM}}(\Omega) = E(\Omega) + mE(\Omega - \omega_m) + mE(\Omega + \omega_m), \tag{3}$$

where m and ω_m are modulation index and microwave angular frequency, respectively.

The FBG in our experiment only works in C-band and is modeled as an optical phase filter given by

$$\Phi(\Omega) = |\Phi(\Omega)|\, e^{-jB_2(\Omega-\Omega_0)^2/2 - jB_3(\Omega-\Omega_0)^3/6}, \tag{4}$$

where $|\Phi(\Omega)|^2$ is a rectangular function approximately, Ω_0 the central angular frequency of the light corresponding to wavelength 1550 nm, B_2 total second-order dispersion and B_3 total third-order dispersion. Then the Fourier transform of complex electrical field after FBG is

$$E_{\mathrm{FBG}}(\Omega) = E_{\mathrm{MZM}}(\Omega)\,\Phi(\Omega). \tag{5}$$

Let

$$T(\Omega) = |\Phi(\Omega)|^2 F(\Omega), \tag{6}$$

where $F(\Omega)$ is the transfer function of optical filter for PSD of light. The frequency-domain optical signal after optical filter is expressed as

$$E_{\mathrm{filter}}(\Omega) = \sqrt{T(\Omega)}\, e^{-j\left[B_2(\Omega-\Omega_0)^2/2 + B_3(\Omega-\Omega_0)^3/6\right]} \times \left[E(\Omega) + mE(\Omega - \omega_m) + mE(\Omega + \omega_m)\right]. \tag{7}$$

With the transfer matrices of 50:50 couplers and VDLs, $E_1(\Omega)$ and $E_2(\Omega)$, the optical signals at two outputs of MZI in spectral domain, can be written as

$$\begin{bmatrix} E_1(\Omega) \\ E_2(\Omega) \end{bmatrix} = \begin{bmatrix} 1 + e^{j\Delta\tau\Omega + j\pi} \\ e^{j\pi/2} + e^{j\Delta\tau\Omega + j\pi/2} \end{bmatrix} \frac{E_{\text{filter}}(\Omega)}{2}, \tag{8}$$

where $\Delta\tau$ is the time delay difference of two arms of MZI.

Neglecting the DC component and small values, the electrical signal generated by one photodetector of the balanced detector corresponding to $E_1(\Omega)$ is

$$\begin{aligned} I_1(\omega) &\propto \left\langle \int_0^{+\infty} E_1(\Omega) E_1^*(\Omega - \omega) d\Omega \right\rangle \\ &\propto e^{j\left(B_2\omega^2/2 - B_3\omega^3/6\right)} \left[\delta(\omega + \omega_m) + \delta(\omega - \omega_m)\right] \left[2H_0(\omega) - e^{j\Delta\tau\Omega_0} H_+(\omega) - e^{-j\Delta\tau\Omega_0} H_-(\omega)\right], \end{aligned} \tag{9}$$

where ω is the angular frequency of microwave signal. $H_0(\omega)$ is defined as

$$\begin{aligned} H_0(\omega) &= \int_0^{+\infty} N'(\Omega) e^{j\left[\left(-B_2\omega + B_3\omega^2/2\right)(\Omega - \Omega_0) - B_3\omega(\Omega - \Omega_0)^2/2\right]} d\Omega \\ &\approx \int_0^{+\infty} N'(\Omega) e^{-j\left[B_2\omega(\Omega - \Omega_0) + B_3\omega(\Omega - \Omega_0)^2/2\right]} d\Omega. \end{aligned} \tag{10}$$

$H_+(\omega)$ and $H_-(\omega)$ are defined as

$$\begin{aligned} H_\pm(\omega) &= \int_0^{+\infty} N'(\Omega) e^{j\left[\left(-B_2\omega + B_3\omega^2/2 \pm \Delta\tau\right)(\Omega - \Omega_0) - B_3\omega(\Omega - \Omega_0)^2/2\right]} d\Omega \\ &\approx \int_0^{+\infty} N'(\Omega) e^{j\left[\left(-B_2\omega \pm \Delta\tau\right)(\Omega - \Omega_0) - B_3\omega(\Omega - \Omega_0)^2/2\right]} d\Omega, \end{aligned} \tag{11}$$

where $N'(\Omega) = T(\Omega)N(\Omega)$. For the FBG ($B_3 = -3.96\,\text{ps}^3$ at 1550 nm) used in our experiment or several tens of kilometers of single-mode fiber (SMF28, $B_3 = \beta_3 L$, where L is fiber length and $\beta_3 = 0.0625\,\text{ps}^3/\text{km}$ at 1540 nm), we obtain $|B_3\omega^2/2| \ll 2\pi$ under the condition that $\omega < 100\,\text{GHz}$, so the term $\exp(jB_3\omega^2/2)$ is close to 1 and can be neglected in (10) and (11).

Since the input microwave signal for MPF in frequency-domain is $\delta(\omega - \omega_m) + \delta(\omega + \omega_m)$, the MPF's transfer function corresponding to $E_1(\Omega)$ is

$$H_1(\omega) \propto e^{j\left(B_2\omega^2/2 - B_3\omega^3/6\right)} \left[2H_0(\omega) - e^{j\Delta\tau\Omega_0} H_+(\omega) - e^{-j\Delta\tau\Omega_0} H_-(\omega)\right]. \tag{12}$$

It is composed of the baseband response and the passband response. Similarly, the MPF's transfer function for another detector of the balanced detector corresponding to $E_2(\Omega)$ is

$$H_2(\omega) \propto e^{j\left(B_2\omega^2/2 - B_3\omega^3/6\right)} \left[2H_0(\omega) + e^{j\Delta\tau\Omega_0} H_+(\omega) + e^{-j\Delta\tau\Omega_0} H_-(\omega)\right]. \tag{13}$$

Finally, the MPF's total transfer function for our system is expressed as

$$H(\omega) \propto e^{j\left(B_2\omega^2/2 - B_3\omega^3/6\right)} \left[e^{j\Delta\tau\Omega_0} H_+(\omega) + e^{-j\Delta\tau\Omega_0} H_-(\omega)\right]. \tag{14}$$

Clearly, our systematical derivation proves that the baseband response is removed and the amplitude of passband response is doubled by balanced detection. Moreover, with the shifted dispersion-induced radio frequency fading effect [4], [6], the center frequency of passband can be tunable by adjusting the time delay difference of two arms of MZI. According to (11), we get $B_2\omega = \pm\Delta\tau$ at the center of passband response. With $\omega = 2\pi f$ and $\Delta\tau = \Delta l/c$, the center frequency of passband response is written as

$$f_0 = \pm\Delta l / 2\pi c B_2, \tag{15}$$

where Δl is optical path difference between two arms of MZI.

Let us consider the effect of third-order dispersion B_3 on passband response in this MPF. In (11), the section $\exp(-jB_3\omega(\Omega - \Omega_0)^2/2)$ could be regarded as a kind of chirp mathematically. Here, we

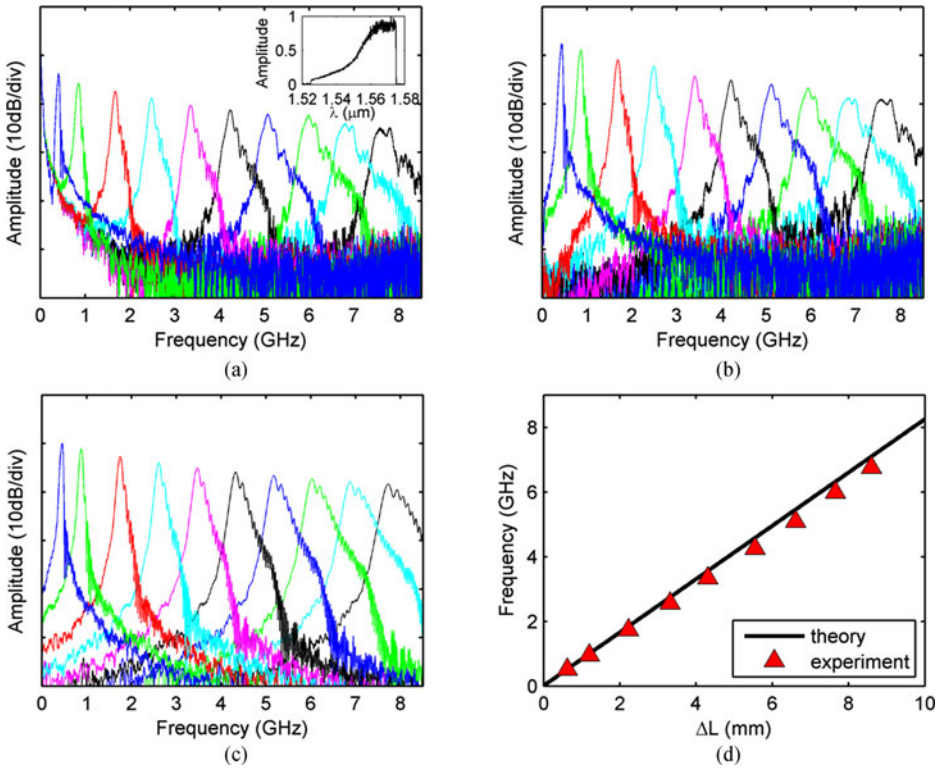

Fig. 2. The frequency responses measured by VNA. The frequency responses with $\Delta l = 0.63$, 1.21, 2.23, 3.32, 4.32, 5.55, 6.62, 7.66, 8.61 and 9.94 mm are correspond to the colored curves from left to right, respectively. (a) without dual balanced detection. The inset shows the optical spectrum after tunable optical filter when measuring all the frequency responses. (b) with dual balanced detection. (c) Theoretical frequency responses obtained by (14). (d) The relationship of center frequency of passband response and optical path difference between two arms of MZI.

discuss two important limiting cases. When $N'(\Omega)$ is very narrow or ω is very small, the chirp section $\exp(-jB_3\omega(\Omega-\Omega_0)^2/2)$ is close to 1, which means it can be neglected. Under this condition, the passband response actually takes the shape of Fourier transform of $N'(\Omega)$. On the other hand, if the chirp is big enough, the passband response will be broadened and take the shape of $N'(\Omega)$. For simplicity, we take an average chirp at the center frequency of passband response, so that the Ω-to-ω mapping law is written as $(\pm\Delta\tau - B_2\omega)/(\Omega-\Omega_0) = B_3\omega \approx \pm B_3\Delta\tau/B_2$ for $H_+(\omega)$ and $H_-(\omega)$ respectively. Then the relationship is expressed as

$$|H_\pm(\omega)| \sim N'\left[B_2\left(\Delta\tau \mp B_2\omega\right)/\left(B_3\Delta\tau\right) + \Omega_0\right]. \tag{16}$$

According to (16), it implies that by changing the shape of $N'(\Omega)$ with the tunable optical filter, the passband response can be modified and even an adjustable notch can be also generated. This is the main conclusion of our theoretical derivation for the system as shown in Fig. 1(a).

3. Results and Discussion

In this section, a comparison between experimental data and numerical results of frequency response is made. Afterwards we further investigate the characteristics of the tunable passband and notch experimentally, respectively.

When using only one input or both two inputs of balanced amplified photodetector, the experimental frequency responses are shown in Fig. 2(a) and (b), respectively. In both cases, by tuning the VDL, the center frequency of passband changes accordingly. In the former case, there is always a baseband at zero frequency, but in the latter case, there is none. Just as the theoretical

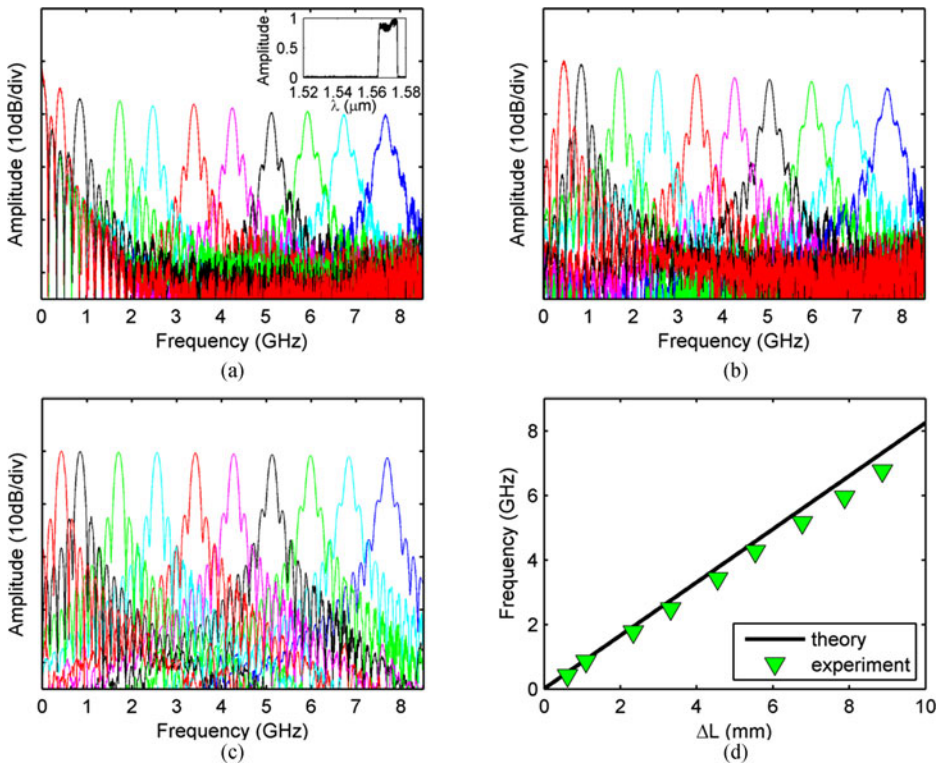

Fig. 3. With a narrow optical spectrum, the frequency responses measured by VNA. The frequency responses with $\Delta l = 0.62, 1.11, 2.34, 3.33, 4.56, 5.55, 6.78, 7.89, 8.87$ and 10.12 mm are correspond to the colored curves from left to right, respectively. (a) without dual balanced detection. The inset shows the optical spectrum after tunable optical filter when measuring all the frequency responses. (b) with dual balanced detection (c) Theoretical frequency responses obtained by (14). (d) The relationship of center frequency of passband response and optical path difference between two arms of MZI.

prediction, the baseband is obviously removed by balanced detection. The peak passband frequency is tuned from 0 to 8.5 GHz by VDL, because the highest measured operating frequency is limited by bandwidth of VNA. The passband response becomes wider when the frequency gets higher, as in Fig. 2(b). With the experimental parameters, the same phenomenon is observed in the simulation results of (14), shown in Fig. 2(c). Thus the experimental results are in good agreement with the simulated frequency responses. Moreover, as in Fig. 2(d), the experimental relationship of center frequency of passband response to optical path difference of MZI and theoretical prediction of (15) also agree well each other.

According to (11), the passband responses in Fig. 2(a) and (b) are broadened due to the chirp section $\exp(-jB_3\omega(\Omega - \Omega_0)^2/2)$. Note that when the passband center frequency is tuned from 0 to 8.5 GHz, the -3 dB bandwidth of the MPF varies from $\sim$60 to $\sim$450 MHz in Fig. 2(a) and (b). Mathematically, this broadening effect has obviously positive correlation with frequency ω and optical bandwidth $\Delta\Omega$. That is why the passband responses in higher frequency are wider. For a narrow optical spectrum filtered by tunable optical filter, which means a small optical spectrum width $\Delta\Omega$, the broadening effect is weak and could even be neglected. In Fig. 3(a) and (b), the passband width is independent of center frequency and keeps a fixed value i.e., $\sim$150 MHz when filtering a narrow optical spectrum as shown in inset. For the almost unchanged width of passband response in simulated results of (14), shown in Fig. 3(c), the experimental results agree theory pretty well. Note that Fig. 3(a) and (b) are obtained when using only one input or both two inputs of balanced photodetector, respectively. Similarly, the baseband response at zero frequency only exists in Fig. 3(a), as baseband is removed by balanced detection. The out-of-band rejection is $\sim$30 dB in Figs. 2(b) and 3(b). The frequency responses of the architectures shown in Fig. 2(a) and (b)

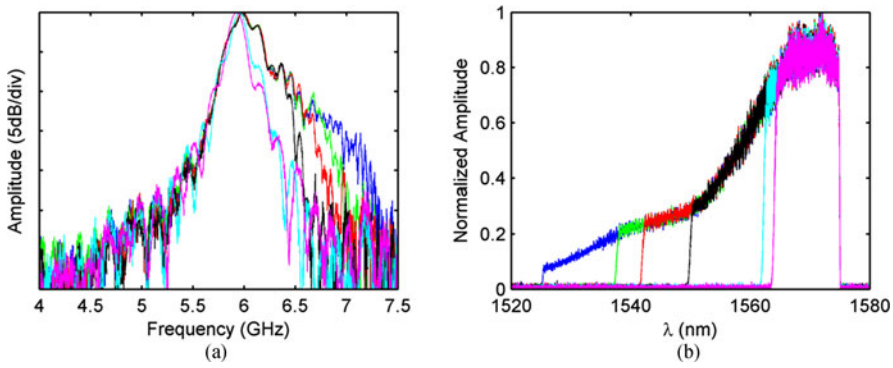

Fig. 4. Change the bandwidth of passband response of MPF with the tunable optical filter. (a) passband response. (b) optical spectrum $N'(\Omega)$.

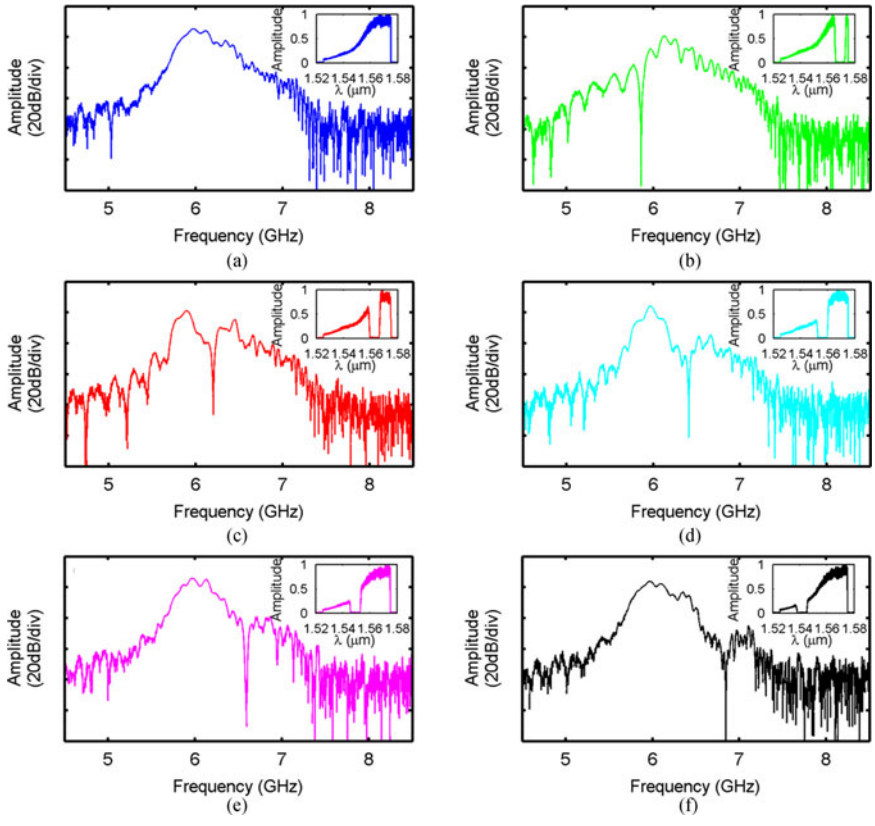

Fig. 5. Change the frequency of notch response by tuning the position of gap in optical spectrum $N'(\Omega)$ with the tunable optical filter. The insets show the optical spectrums after tunable optical filter.

and Fig. 3(a) and (b) are measured under $B_2 = 643.4136\,\text{ps}^2$, $B_3 = -3.96\,\text{ps}^3$. In addition, (15) is confirmed again by experiment, as shown in Fig. 3(d).

Fig. 4(a) shows the continuous variation of passband response of MPF when tuning the optical filter. The corresponding optical spectrums are shown in Fig. 4(b). The -3 dB bandwidth of passband response of MPF could vary from $\sim$330 MHz to $\sim$150 MHz continuously, as in Fig. 4(a). According to (16), when the optical spectrum is relatively wide, the passband response of MPF takes the shape of optical spectrum. In experiment, the optical spectrum is irregular due to the mismatch of the operating wavelength range of FBG and the optical spectrum of SLD. This results in the degraded MPF response and its roll-off in Fig. 4(a). To solve this problem in practical use and improve the

MPF performance, a light source with a rectangular optical spectrum such as the ASE source could be used.

By replacing the blocker with a movable metal wire as a spatial filter in tunable optical filter, we generate a notch both in optical spectrum and passband response of MPF. When tuning the position of the metal wire, the notch in optical spectrum/passband response moves accordingly and continuously. For the passband response shown in Fig. 5(a), the frequency of notch response is adjusted to be 5.86, 6.21, 6.41, 6.59 and 6.85 GHz, respectively, as in Fig. 5(b)–(f). The insets show the corresponding optical spectrums.

4. Conclusion

In summary, a baseband-free band-pass MPF with continuously tunable center frequency and bandwidth has been presented. The center frequency was tuned from 0 to 8.5 GHz experimentally, which can be even much higher but limited by operating frequency range of VNA used here. In addition, the −3 dB bandwidth of passband response of this MPF could vary from ∼330 MHz to ∼150 MHz continuously. Furthermore, a continuously tunable notch could be produced in this band-pass MPF by making a movable gap in optical spectrum with tunable optical filter. Different from previous designs, the proposed MPF requires only one light source without the need of temperature controller and/or AWG.

Acknowledgment

The authors would like to thank Prof. B. Wei for his helpful discussion and technical support.

References

[1] J. Capmany, B. Ortega, and D. Pastor, "A tutorial on microwave photonic filters," *J. Lightw. Technol.*, vol. 24, no. 1, pp. 201–229, Jan. 2006.
[2] H. Wang *et al.*, "Widely tunable single-bandpass microwave photonic filter based on polarization processing of a nonsliced broadband optical source," *Opt. Lett.*, vol. 38, no. 22, pp. 4857–4860, Nov. 2013.
[3] J. Ge and M. P. Fok, "Passband switchable microwave photonic multiband filter," *Sci. Rep.*, vol. 5, 2015, Art. no. 15882.
[4] J. Mora *et al.*, "Photonic microwave tunable single-bandpass filter based on a Mach-Zehnder interferometer," *J. Lightw. Technol.*, vol. 24, no. 7, pp. 2500–2509, Jul. 2006.
[5] X. X. Xue, X. P. Zheng, H. Y. Zhang, and B. K. Zhou, "Widely tunable single-bandpass microwave photonic filter employing a non-sliced broadband optical source," *Opt. Exp.*, vol. 19, no. 19, pp. 18423–18429, Sep. 2011.
[6] L. W. Li, X. K. Yi, T. X. H. Huang, and R. A. Minasian, "Shifted dispersion-induced radio-frequency fading in microwave photonic filters using a dual-input Mach–Zehnder electro-optic modulator," *Opt. Lett.*, vol. 38, no. 7, pp. 1164–1166, Apr. 2013.
[7] T. Chen, X. K. Yi, L. W. Li, and R. Minasian, "Single passband microwave photonic filter with wideband tunability and adjustable bandwidth," *Opt. Lett.*, vol. 37, no. 22, pp. 4699–4701, Nov. 2012.
[8] W. Li, C. W. Yang, L. Wang, J. G. Liu, and N. H. Zhu, "Single-notch microwave photonic filter using a nonsliced ASE source and a laser diode," *IEEE Photon. J.*, vol. 8, no. 1, Feb. 2016, Art. no. 5500207.
[9] M. Ziyadi *et al.*, "Tunable radio frequency photonics filter using a comb-based optical tapped delay line with an optical nonlinear multiplexer," *Opt. Lett.*, vol. 40, no. 14, pp. 3284–3287, Jul. 2015.
[10] Y. Yu, S. Y. Li, X. P. Zheng, H. Y. Zhang, and B. K. Zhou, "Tunable microwave photonic notch filter based on sliced broadband optical source," *Opt. Exp.*, vol. 23, no. 19, pp. 24308–24316, Sep. 2015.
[11] W. Li *et al.*, "Microwave photonic bandstop filter with wide tunability and adjustable bandwidth," *Opt. Exp.*, vol. 23, no. 26, pp. 33579–33586, Dec. 2015.
[12] Y. Stern *et al.*, "Tunable sharp and highly selective microwave-photonic band-pass filters based on stimulated Brillouin scattering," *Photon. Res.*, vol. 2, pp. B18–B25, Aug. 2014.
[13] W. Wei, L. Yi, Y. Jaouën, M. Morvan, and W. Hu, "Brillouin rectangular optical filter with improved selectivity and noise performance," *IEEE Photon. Technol. Lett.*, vol. 27, no. 15, pp. 1593–1596, Aug. 2015.
[14] A. Choudhary *et al.*, "Tailoring of the Brillouin gain for on-chip widely tunable and reconfigurable broadband microwave photonic filters," *Opt. Lett.*, vol. 41, no. 3, pp. 436–439, Feb. 2016.
[15] R. Wu, M. Song, D. E. Leaird, and A. M. Weiner, "Comb-based radio-frequency photonic filtering with 20 ns bandwidth reconfiguration," *Opt. Lett.*, vol. 38, no. 15, pp. 2735–2738, Aug. 2013.
[16] J. H. Lee and Y. M. Chang, "Detailed theoretical and experimental study on single passband, photonic microwave fir filter using digital micromirror device and continuous-wave supercontinuum," *J. Lightw. Technol.*, vol. 26, no. 15, pp. 2619–2628, Aug. 2008.
[17] D. Guang-Hua and E. Georgiev, "Non-white photodetection noise at the output of an optical amplifier: theory and experiment," *IEEE J. Quantum Electron.*, vol. 37, no. 8, pp. 1008–1014, Aug. 2001.